

Space Robotics

Space System Design, MAE 342, Princeton University
Robert Stengel

- Robots and Robotics
- Autonomous Spacecraft
- Planetary and Lunar Rovers
- Path Planning
- Robotic Arms
- Robonauts
- Deep Impact 1

*Copyright 2016 by Robert Stengel. All rights reserved. For educational use only.
<http://www.princeton.edu/~stengel/MAE342.html>*

1



Robots and Robotics

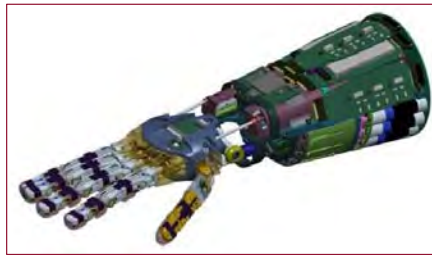


- Design, manufacture, control, and programming of robots
- Use of robots to solve problems
- Study of control processes, sensors, and algorithms used in humans, animals, and machines
- Application of control processes and algorithms to designing robots

2

Biomimetics (Bionics)

- Understanding biological principles and applying them to system design
 - Configuration
 - Structure
 - Behavior
 - Dynamics
 - Control



3

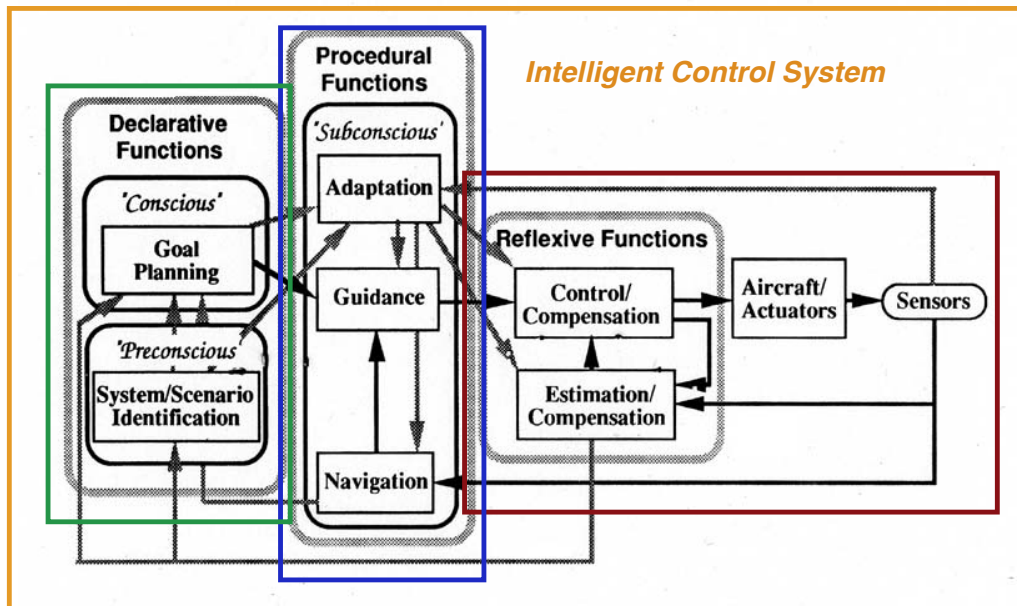
Autonomous Robots

- Self control
- Self maintenance
- Awareness of environment
- Task orientation
- Mission specificity
- Power source
- Cooperation and collaboration
- = Intelligence?
- Self replication?
- Ethical issues



4

Elements of Intelligent Control



Declarative Functions
Procedural Functions
Reflexive Functions

Expert Systems, Decision Trees
Estimation and Control "Circuits"
Control Laws, Neural Networks

5

Robotic Vehicles

6



Expendable (Rocket) Launch Vehicles

Current space launch vehicles are largely autonomous



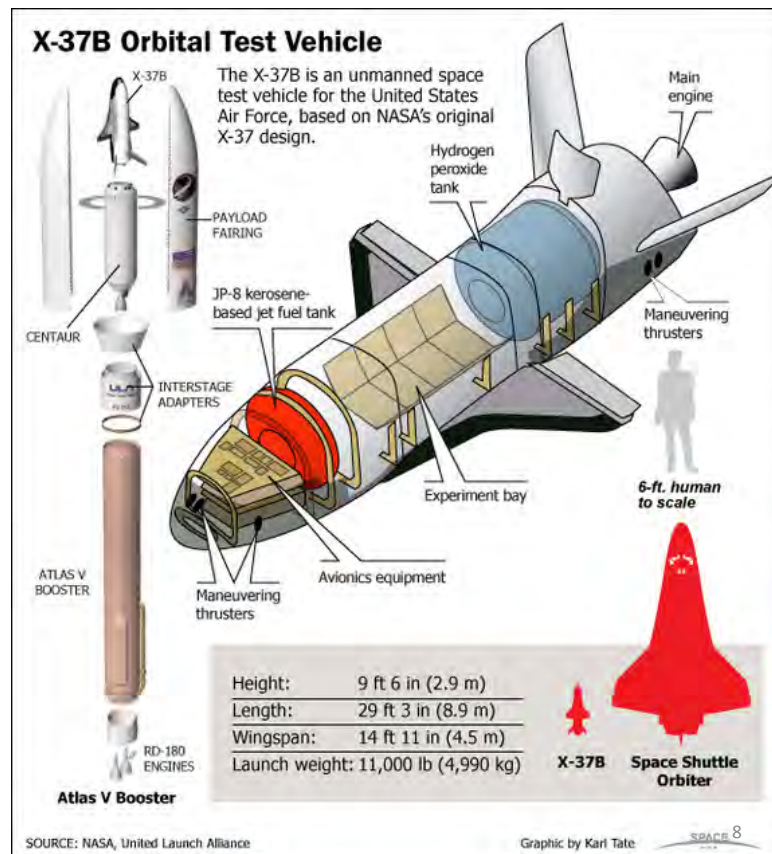
Atlas V

<http://www.youtube.com/watch?v=KxQbex7LJwg>

7

X-37B

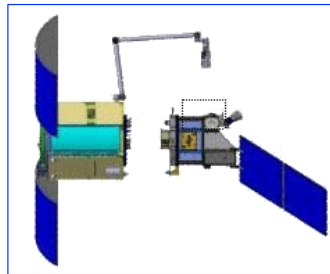
- Reusable experimental/operational vehicle
- Unmanned “mini-Space Shuttle”
- Highly classified project
- 1st 3 missions: 224, 469, & 675 days in orbit
- 4th mission on-going



Orbital Express: ASTRO and NEXTSat



- **DARPA, 2007**
 - Automatic rendezvous, docking, and undocking
 - On-orbit transfer of replaceable units
 - 6DOF robot arm
 - Video guidance sensor
 - Atlas 5 launch

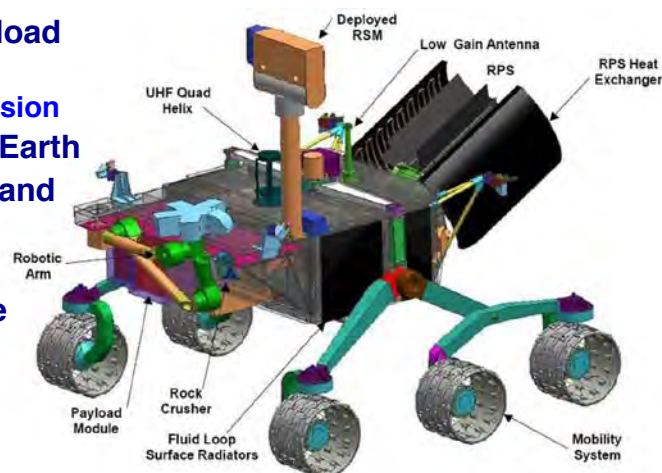


https://en.m.wikipedia.org/wiki/Robotic_spacecraft

9

Mars Science Laboratory (Curiosity)

- Transport science payload over Martian surface
 - Rocker-bogie suspension
- Communications with Earth
- Guidance, navigation, and control
- Power supply
- Support for deployable devices
- Size ~ Mini-Cooper
- Landed, 8/6/12, and operational

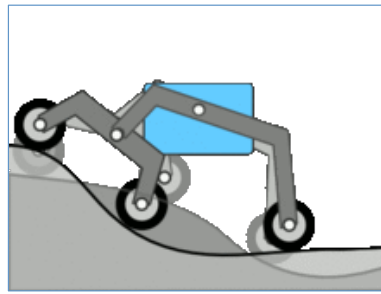


Curiosity Trailer

<http://www.jpl.nasa.gov/video/details.php?id=1014>

10

Curiosity Rocker-Bogie Suspension

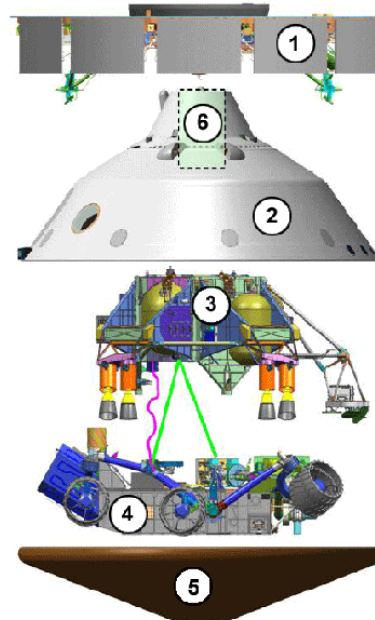


Curiosity Robotic Arms



11

Curiosity Preparation, Spacecraft, and Aeroshell



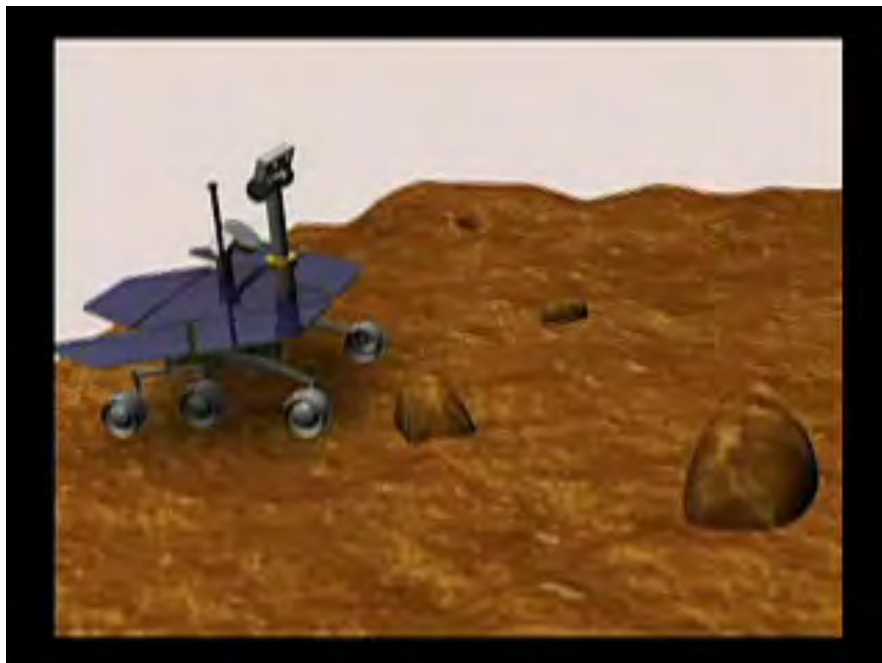
12

Curiosity Approach and Landing



13

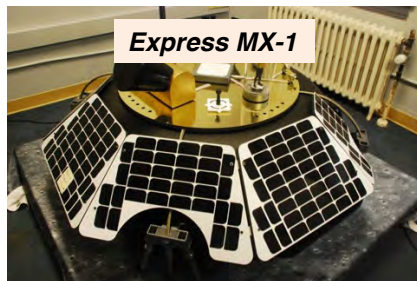
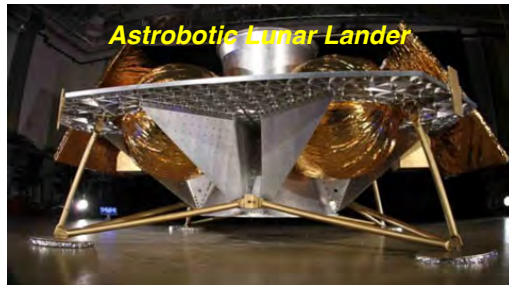
Mars Opportunity Rover Navigation



14

Google LunarX Prize

1st privately funded spacecraft to land on Moon, travel 500m, and stream live TV

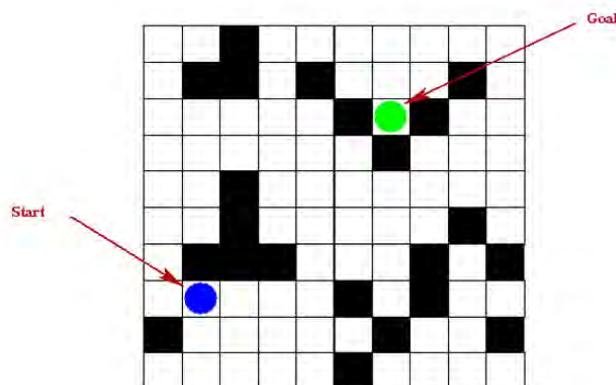


https://en.m.wikipedia.org/wiki/Google_Lunar_X_Prize

15

Path Planning on Occupancy Grid

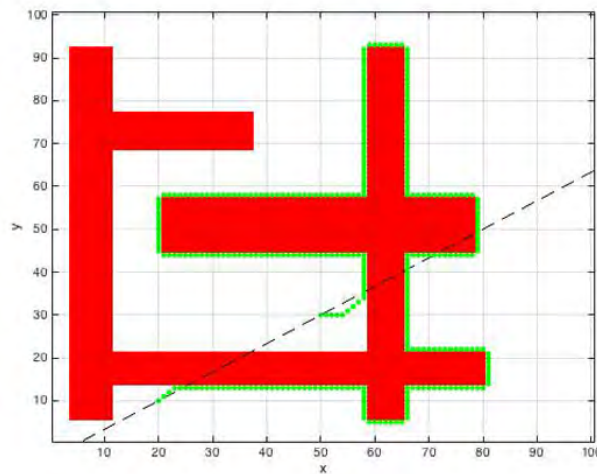
Admissible and Inadmissible Blocks



- Identify feasible paths from Start to Goal
- Chose path that best satisfies criteria, e.g.,
 - Simplicity of calculation
 - Lowest cost
 - Highest performance

16

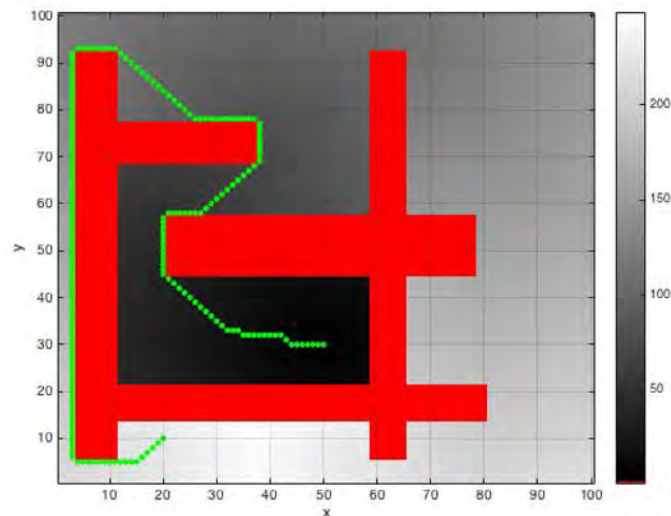
Bug Path Planning



- 1) Identify shortest unconstrained path from Start to Goal
- 2) Chose path that navigates the boundary
 - 1) Stays as close as possible to unconstrained path
 - 2) Satisfies constraint
 - 3) Follows simple rule, e.g., “stay to the left”

17

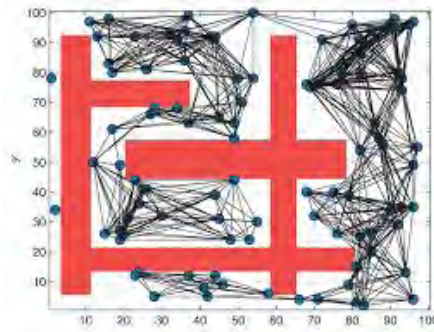
D* or A* Path Planning



- Determine occupancy cost of each block
- Chose path from Start to Goal that **minimizes occupancy cost with each step**

18

Probabilistic Road Map

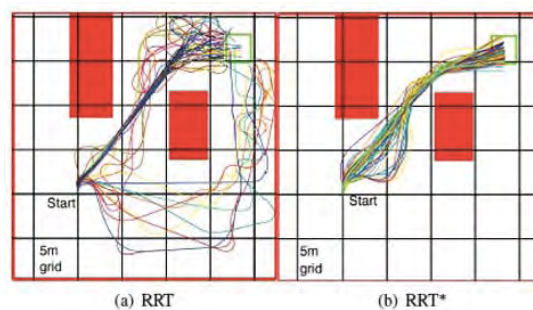


- **Construction Phase:** Random configuration of admissible points
 - Connect admissible points to nearest neighbors
- **Assessment Phase:** Assess incremental cost of traveling along each “edge” between points
- **Query Phase:** Find all feasible paths from Start to Goal and select lowest cost path

Note that this approach would miss the lowest cost path found on the previous slide

19

Rapidly Exploring Random Trees (RRT, RRT*)

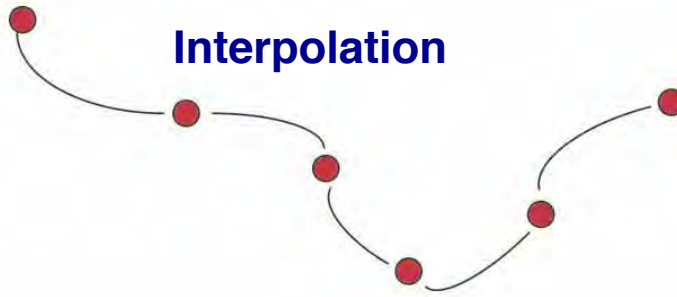


- **RRT**
 - Space-filling tree evolves from Start
 - Open-loop trajectories with state constraints
 - Initially feasible solution converges to optimal solution through searching
- **RRT***
 - “Committed trajectories”
 - Branch-and-bound tree adaptation
 - Provable convergence

20

Connect the Dots

Interpolation

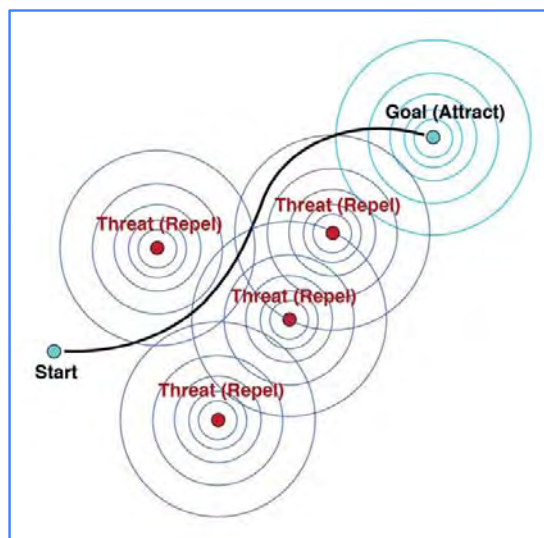


- Piecewise polynomials (linear \rightarrow quintic)
 - End-point discontinuities
 - End-point constraints
- Single polynomial through all points
 - Polynomial degree = # of points $- 1$
 - Sensitivity to high-degree terms (e.g., ct^6)
 - Possibility of large excursions between points
- Polynomials through adjacent points
 - e.g., cubic B splines

21

Path Planning with Potential Fields

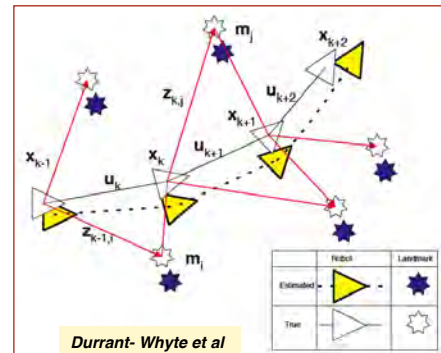
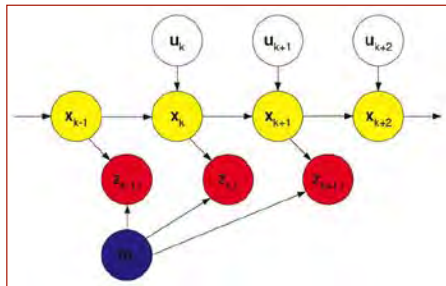
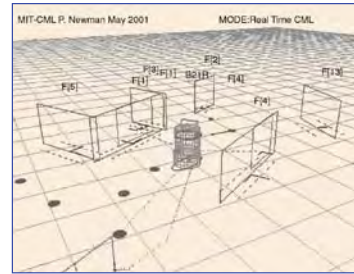
Features attract or repel path from Start to Goal, e.g., \pm gravity fields



22

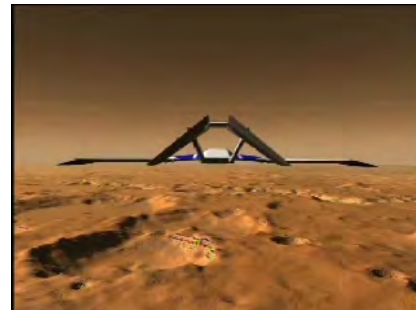
Simultaneous Location and Mapping (SLAM)

- Build or update a local map within an unknown environment
 - Stochastic map, defined by mean and covariance of many points
 - Landmark, terrain, and target tracking
 - Multi-sensor integration
 - SLAM Algorithm = Bank of state estimators



23

Mars Aerial Regional-Scale Environmental Survey (ARES) Research Airplane Concept, ~2008



<https://www.youtube.com/watch?v=8YutbpJuFil>

<https://www.youtube.com/watch?v=wAOTomGFs5M>

24

ARES System Layout

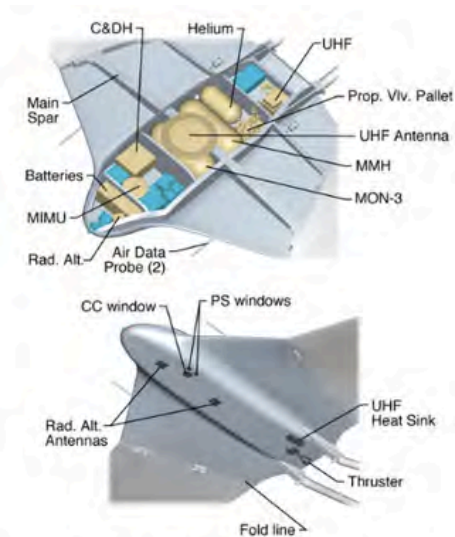


Figure 7: ARES Subsystem Layout.

Table 3: Airplane Mass and Performance Summary			
	Airplane Design		
	Current Best Estimate	Growth	Allocation
Airplane dry mass (kg)	82	101	127
Propellant mass (kg)	48	48	48
Airplane wet mass (kg)	130	149	175
Range, km	680	600	500
Endurance, min	81	71	60

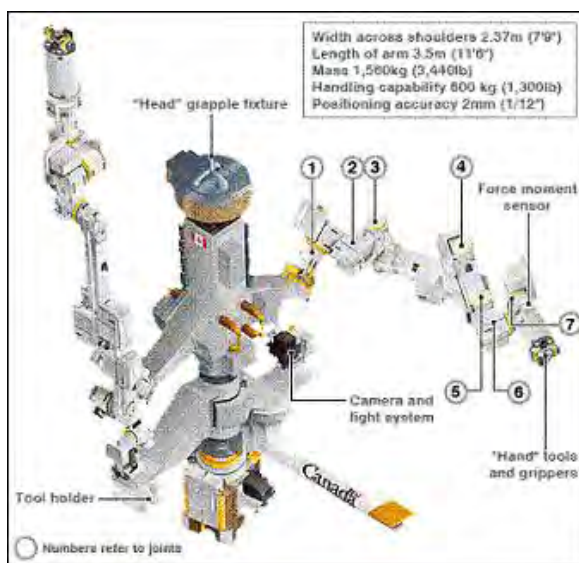
Articulated Robot Arms

Robot Arms for Space

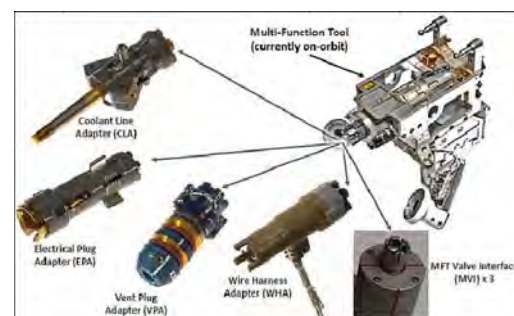


27

DEXTRE

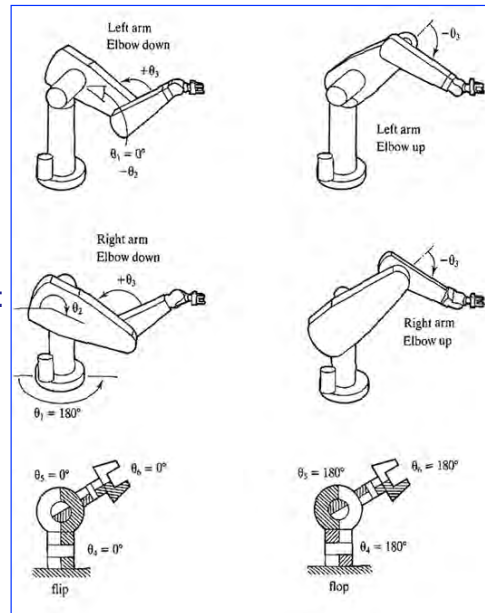
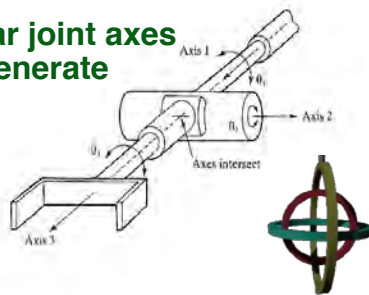


Dextre Specifications	
Height	12 feet
Width	7.7 feet (across shoulders)
Arm Length	11.48 feet linear stroke
Mass (approx.)	3,664 pounds
Mass Handling/Transportation Capacity	1,322.77 pounds
Degrees of Freedom	15
Peak Power (operational)	2,000 W
Avg. Power (keep alive)	600 W
Applied Tip Load Range	0-111 N
Stopping Distance (under max. load)	5.9 inches



Manipulator Redundancy and Degeneracy

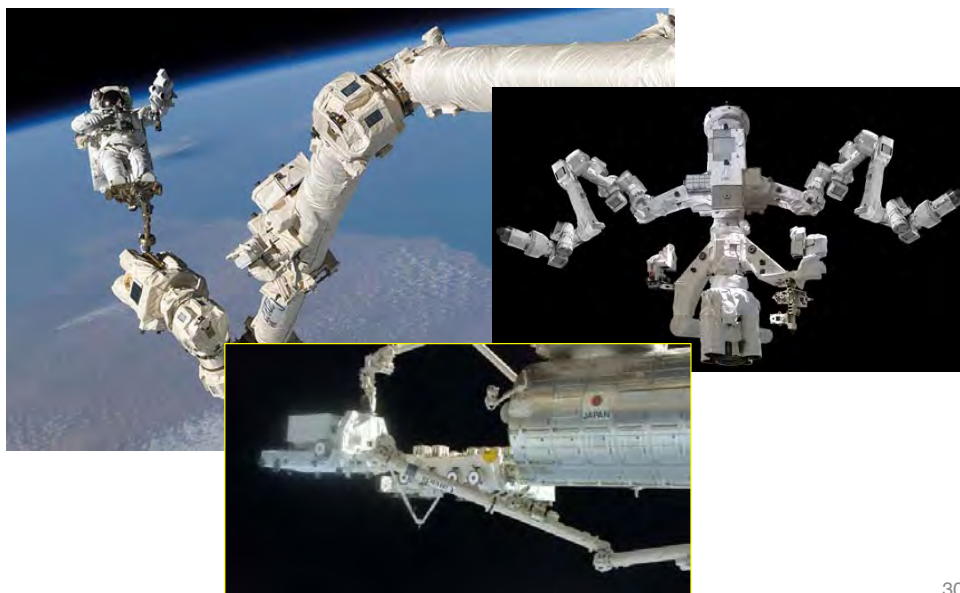
- More than one link configuration may provide a given end point if $\dim(x_J) \geq \dim(x_E) \geq \dim(x_T)$
- **Redundancy**: Finite number of joint vectors provide the same task-dependent vector
- **Degeneracy**: Infinite number of joint vectors provide the same task-dependent vector
- **Co-linear joint axes are degenerate**



29

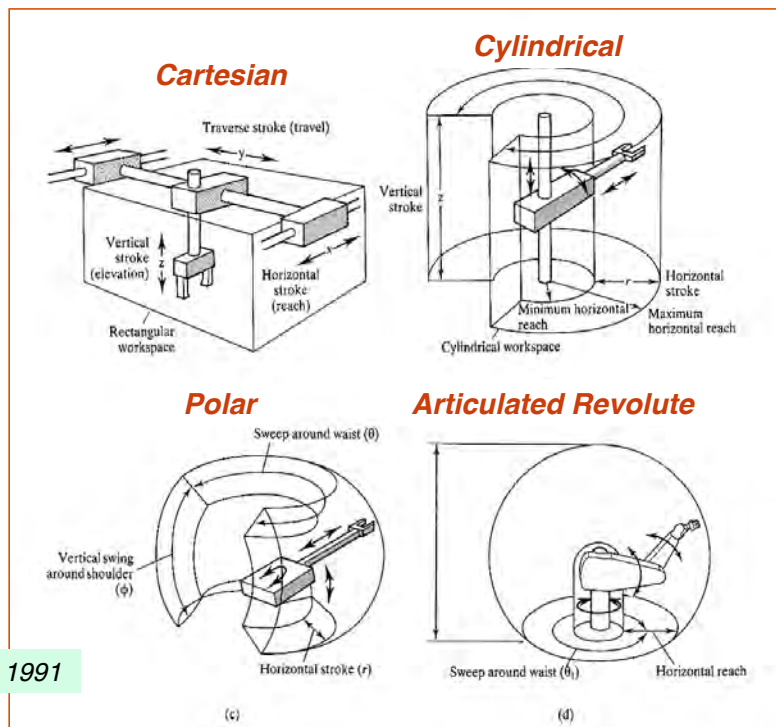
Space Robot Arms are Highly Redundant

Why?



30

Robot Arm Configurations

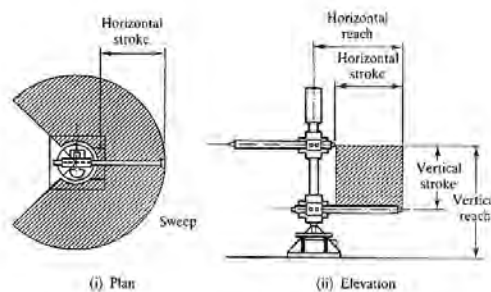


McKerrow, 1991

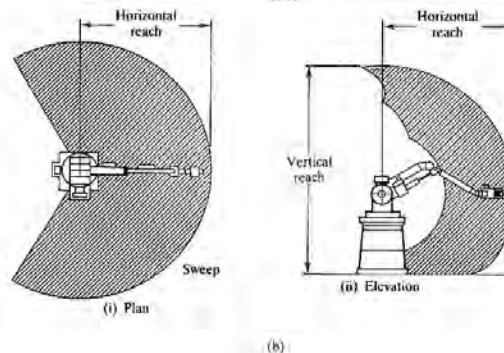
31

Robot Arm Workspaces

Cylindrical



Articulated Revolute



McKerrow, 1991

32

Serial Robotic Manipulators

Proximal link: closer to the base

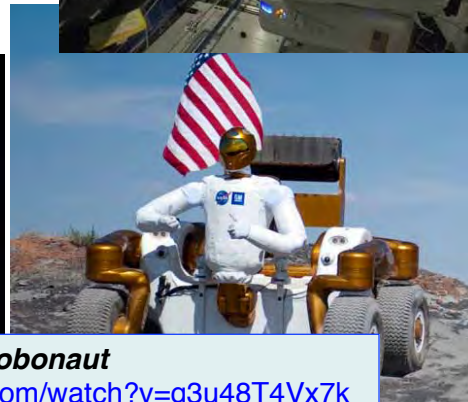
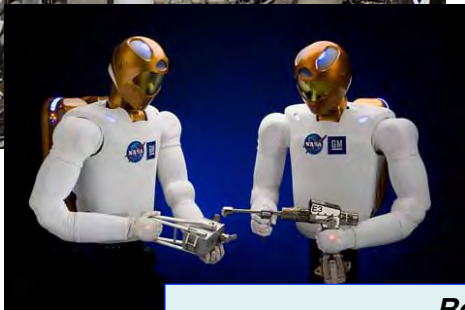
Distal link: farther from the base

- Serial chain of robotic links and joints
 - Large workspace
 - Low stiffness
 - Cumulative errors from link to link
 - Proximal links carry the weight and load of distal links
 - Actuation of proximal joints affects distal links
 - Limited load-carrying capability at end effector



33

NASA/GM Robonaut R2

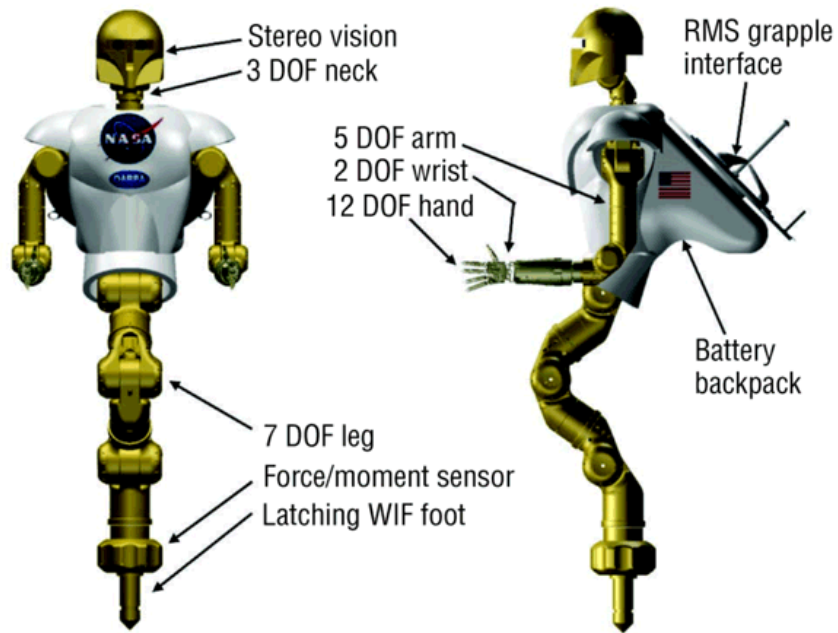


Robonaut

<http://www.youtube.com/watch?v=g3u48T4Vx7k>

34

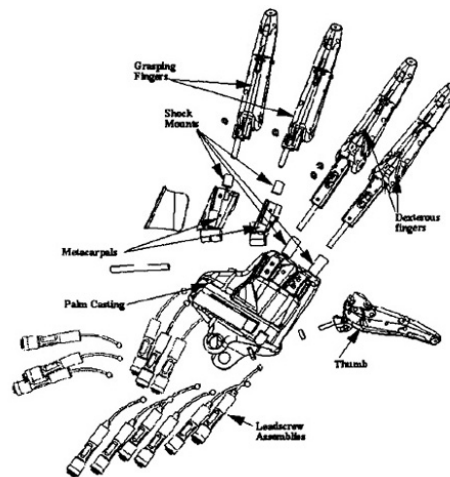
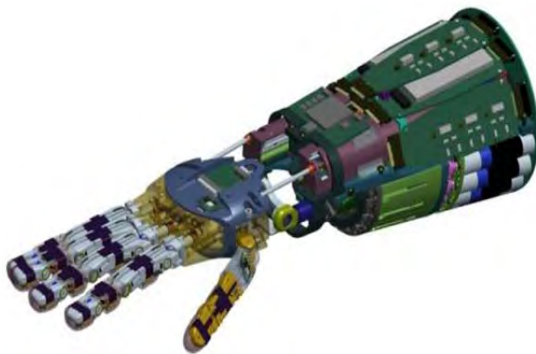
Robonaut 2 Structure



35



Robonaut 2 Hand



36

Robonaut 2 Fingers

Index Finger

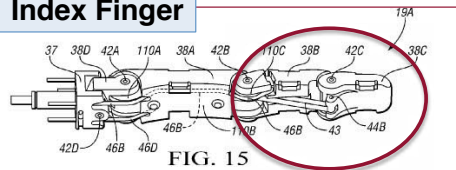


FIG. 15

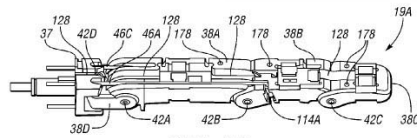


FIG. 16

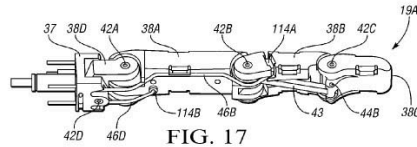
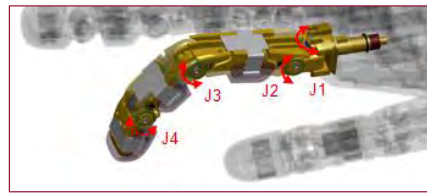


FIG. 17



Thumb

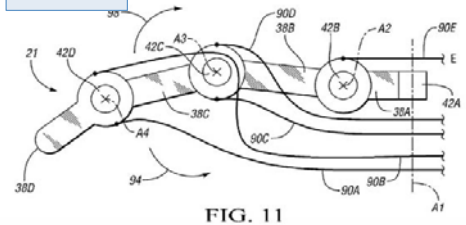


FIG. 11

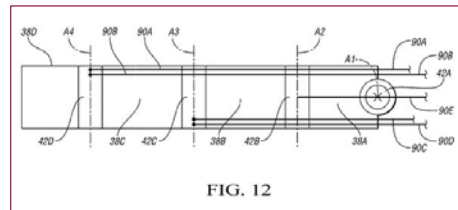


FIG. 12

- Control by tendons and four-bar linkages
- Linear actuators in forearm

37

Four-Bar Linkage

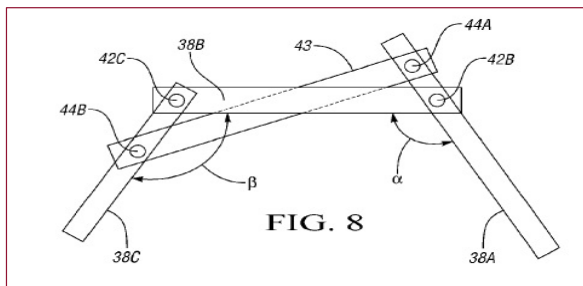
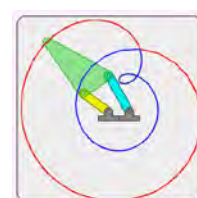
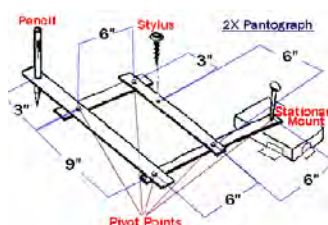
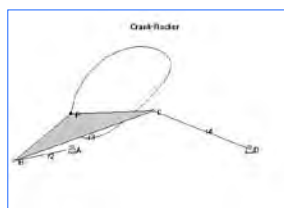


FIG. 8

- Closed-loop structure
- Rotational joints
- Planar motion
- Proportions of link lengths determine pattern of motion



38

Robonaut 2 Wrist and Forearm

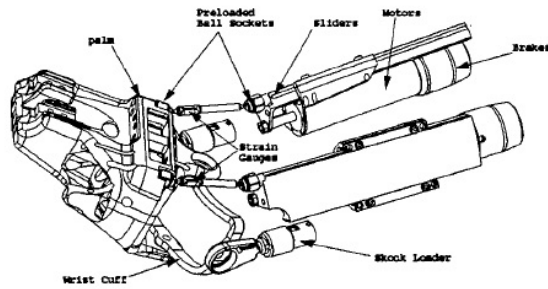


Figure 9 Wrist mechanism

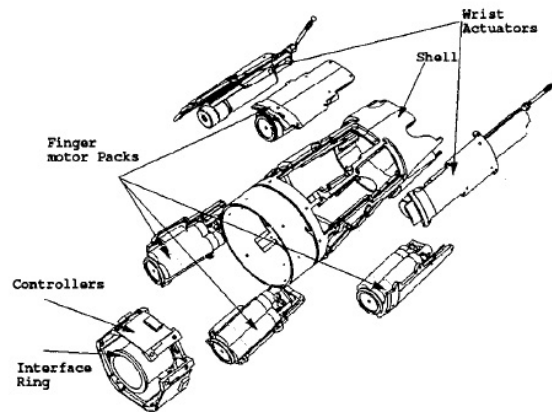
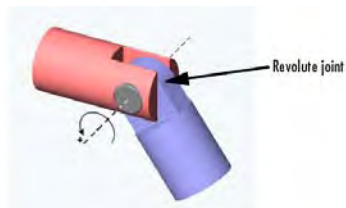


Figure 10: Forearm

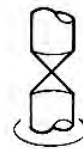
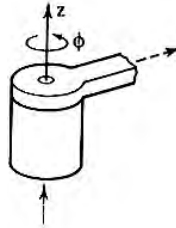
39



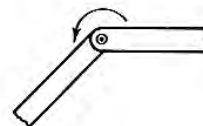
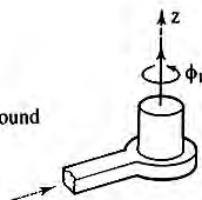
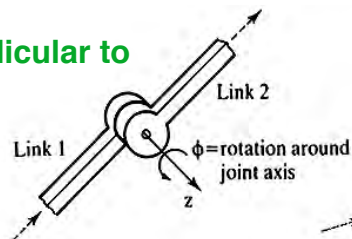
Revolute Robotic Joints

Rotation about a single axis

Parallel to
Link



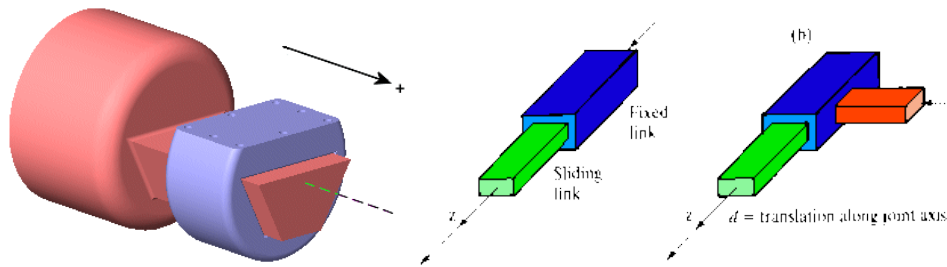
Perpendicular to
Link



40

Prismatic Robotic Joints

Sliding along a single axis



41

Universal



Other Robotic Joints

Constant-Velocity



Flexible



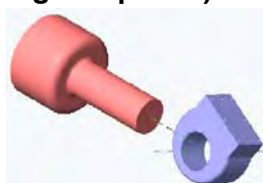
Spherical (or ball)



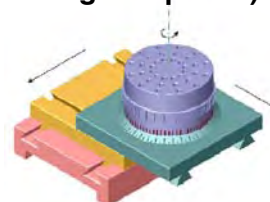
Roller Screw



Cylindrical (sliding and turning composite)



Planar (sliding and turning composite)

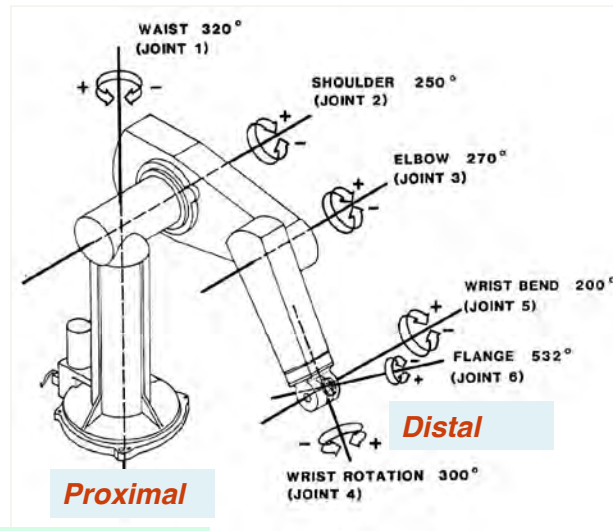


42

Characteristic Transformation of a Link

Link: solid structure between two joints

- Each link type has a **characteristic transformation matrix** relating the proximal joint to the distal joint
- Link n has
 - **Proximal end**: Joint n , coordinate frame $n-1$
 - **Distal end**: Joint $n+1$, coordinate frame n



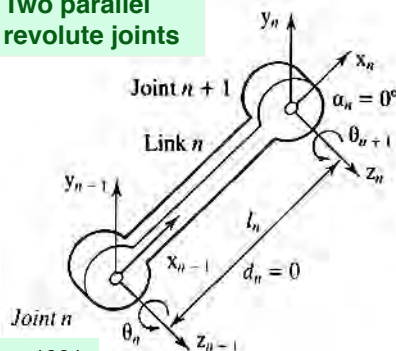
McKerrow, 1991

43

Links Between Revolute Joints

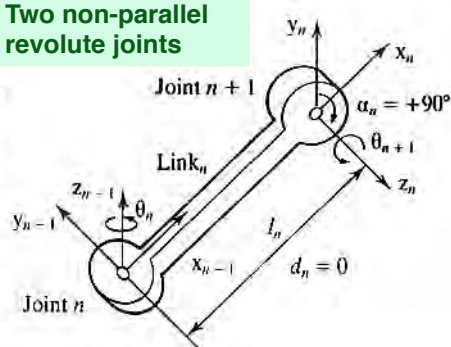
- Link: solid structure between two joints
 - Proximal end: closer to the base
 - Distal end: farther from the base
- **4 Link Parameters**
 - Length of the link between rotational axes, l , along the common normal
 - Twist angle between axes, α
 - Angle between 2 links, θ (revolute)
 - Offset between links, d (prismatic)
- **Joint Variable**: single link parameter that is free to vary

Type 1 Link
Two parallel revolute joints



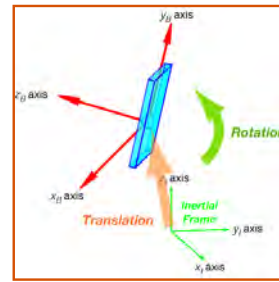
McKerrow, 1991

Type 2 Link
Two non-parallel revolute joints



44

Homogeneous Transformation Matrix



Express rotation and translation in a single transformation

$$\mathbf{s}_{new} = \left[\begin{array}{c|c} \left(\begin{array}{c} \text{Rotation} \\ \text{Matrix} \end{array} \right)_{old}^{new} & \left(\begin{array}{c} \text{Location} \\ \text{of Old} \\ \text{Origin} \end{array} \right)_{new} \\ \hline \left(\begin{array}{ccc} 0 & 0 & 0 \end{array} \right) & 1 \end{array} \right] \mathbf{s}_{old} = \mathbf{A}_{old}^{new} \mathbf{s}_{old}$$

$$(4 \times 1)_{new} = \left[\begin{array}{c|c} (3 \times 3) & (3 \times 1) \\ \hline (1 \times 3) & (1 \times 1) \end{array} \right] (4 \times 1)_{old} = [(4 \times 4)] (4 \times 1)_{old}$$

45

Homogeneous Transformation

- **Rotation and translation can be expressed in terms of homogeneous coordinates**
 - **Single matrix-vector product produces rotation and transformation**

$$\mathbf{s}_{new} = \left[\begin{array}{c|c} H_{old}^{new} & \mathbf{r}_{old_{new}} \\ \hline \left(\begin{array}{ccc} 0 & 0 & 0 \end{array} \right) & 1 \end{array} \right] \mathbf{s}_{old} = \mathbf{A} \mathbf{s}_{old}$$

- **or**

$$\begin{bmatrix} x \\ y \\ z \\ 1 \end{bmatrix}_{new} = \left[\begin{array}{ccc|c} h_{11} & h_{12} & h_{13} & x_o \\ h_{21} & h_{22} & h_{23} & y_o \\ h_{31} & h_{32} & h_{33} & z_o \\ \hline 0 & 0 & 0 & 1 \end{array} \right] \begin{bmatrix} x \\ y \\ z \\ 1 \end{bmatrix}_{old}$$

46

Equivalent Scalar Equations for Homogeneous Transformation

$$\mathbf{s}_{new} = \mathbf{A}_{old}^{new} \mathbf{s}_{old}$$

Matrix-Vector
Multiplication

$$\begin{bmatrix} x \\ y \\ z \\ 1 \end{bmatrix}_{new} = \begin{bmatrix} h_{11} & h_{12} & h_{13} & x_o \\ h_{21} & h_{22} & h_{23} & y_o \\ h_{31} & h_{32} & h_{33} & z_o \\ 0 & 0 & 0 & 1 \end{bmatrix} \begin{bmatrix} x \\ y \\ z \\ 1 \end{bmatrix}_{old}$$

Individual
Operations

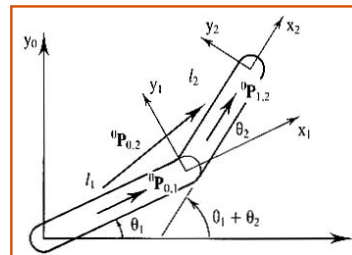
$$\begin{aligned} x_{new} &= h_{11}x_{old} + h_{12}y_{old} + h_{13}z_{old} + x_o \\ y_{new} &= h_{21}x_{old} + h_{22}y_{old} + h_{23}z_{old} + y_o \\ z_{new} &= h_{31}x_{old} + h_{32}y_{old} + h_{33}z_{old} + z_o \\ &\text{---} \\ 1 &= 1 \end{aligned}$$

47

Series of Homogeneous Transformations

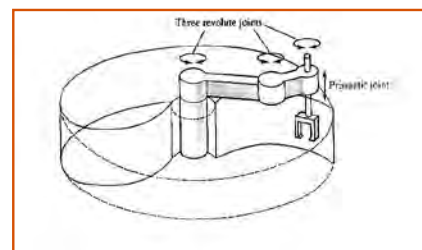
Two serial transformations
can be combined in a single
transformation

$$\mathbf{s}_2 = \mathbf{A}_1^2 \mathbf{A}_0^1 \mathbf{s}_0 = \mathbf{A}_0^2 \mathbf{s}_0$$



Four transformations
for SCARA robot

$$\mathbf{s}_4 = \mathbf{A}_3^4 \mathbf{A}_2^3 \mathbf{A}_1^2 \mathbf{A}_0^1 \mathbf{s}_0 = \mathbf{A}_0^4 \mathbf{s}_0$$



48

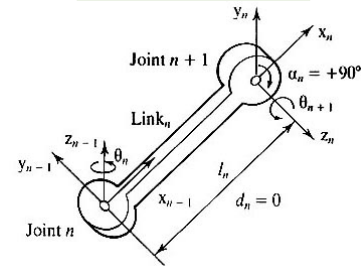
Transformation for a Single Robotic Joint

- Each joint requires four sequential transformations:

- Rotation about α
- Translation along d
- Translation along l
- Rotation about θ

$$\begin{aligned} \mathbf{s}_{n+1} &= \mathbf{A}_3^{n+1} \mathbf{A}_2^3 \mathbf{A}_1^2 \mathbf{A}_n^1 \mathbf{s}_n = \mathbf{A}_n^{n+1} \mathbf{s}_n \\ &= \mathbf{A}_\theta \mathbf{A}_d \mathbf{A}_l \mathbf{A}_\alpha \mathbf{s}_n = \mathbf{A}_n^{n+1} \mathbf{s}_n \end{aligned}$$

Type 2 Link



- ... axes for each transformation (along or around) must be specified

4th

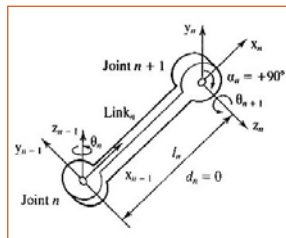
3rd

2nd

1st

$$\mathbf{s}_{n+1} = \mathbf{A}(z_{n-1}, \theta_n) \mathbf{A}(z_{n-1}, d_n) \mathbf{A}(x_{n-1}, l_n) \mathbf{A}(x_{n-1}, \alpha_n) \mathbf{s}_n = \mathbf{A}_n^{n+1} \mathbf{s}_n$$

49



Denavit-Hartenberg Representation of Joint-Link-Joint Transformation

Then

Then

Then

First

$$\mathbf{A}_n = \begin{bmatrix} \cos \theta_n & -\sin \theta_n & 0 & 0 \\ \sin \theta_n & \cos \theta_n & 0 & 0 \\ 0 & 0 & 1 & 0 \\ 0 & 0 & 0 & 1 \end{bmatrix} \begin{bmatrix} 1 & 0 & 0 & 0 \\ 0 & 1 & 0 & 0 \\ 0 & 0 & 1 & d_n \\ 0 & 0 & 0 & 1 \end{bmatrix} \begin{bmatrix} 1 & 0 & 0 & l_n \\ 0 & 1 & 0 & 0 \\ 0 & 0 & 1 & 0 \\ 0 & 0 & 0 & 1 \end{bmatrix} \begin{bmatrix} 1 & 0 & 0 & 0 \\ 0 & \cos \alpha_n & -\sin \alpha_n & 0 \\ 0 & \sin \alpha_n & \cos \alpha_n & 0 \\ 0 & 0 & 0 & 1 \end{bmatrix}$$

$$\mathbf{A}_n = \begin{bmatrix} \cos \theta_n & -\sin \theta_n \cos \alpha_n & \sin \theta_n \sin \alpha_n & l_n \cos \theta_n \\ \sin \theta_n & \cos \theta_n \cos \alpha_n & -\cos \theta_n \sin \alpha_n & l_n \sin \theta_n \\ 0 & \sin \alpha_n & \cos \alpha_n & d_n \\ 0 & 0 & 0 & 1 \end{bmatrix}$$

50

Forward and Inverse Transformations

Forward transformation through links
requires pre-multiplication of matrices

$$\mathbf{s}_1 = \mathbf{A}_0^1 \mathbf{s}_0 \quad ; \quad \mathbf{s}_2 = \mathbf{A}_1^2 \mathbf{s}_1 = \mathbf{A}_1^2 \mathbf{A}_0^1 \mathbf{s}_0 = \mathbf{A}_0^2 \mathbf{s}_0$$

Reverse transformation uses the **matrix inverse**

$$\mathbf{s}_0 = \left(\mathbf{A}_0^2 \right)^{-1} \mathbf{s}_2 = \mathbf{A}_2^0 \mathbf{s}_2 = \mathbf{A}_1^0 \mathbf{A}_2^1 \mathbf{s}_2$$

51

Homogeneous Transformation Matrix is not Orthonormal

$$\mathbf{A}_2^0 = \left(\mathbf{A}_0^2 \right)^{-1} \neq \left(\mathbf{A}_0^2 \right)^T$$

...but a useful identity makes inversion simple

52

Matrix Inverse Identity

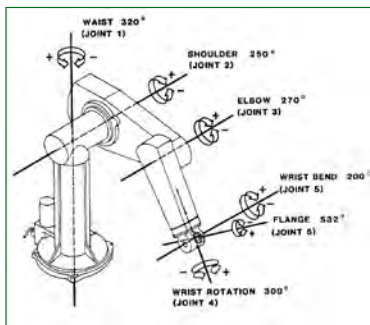
Forward transformation

$$\begin{bmatrix} \mathbf{A}_1 & \mathbf{A}_2 \\ \mathbf{A}_3 & \mathbf{A}_4 \end{bmatrix} = \begin{bmatrix} \mathbf{H}_{old}^{new} & \mathbf{r}_o \\ (0 & 0 & 0) & 1 \end{bmatrix}$$

Inverse

$$\begin{bmatrix} \mathbf{A}_1 & \mathbf{A}_2 \\ \mathbf{A}_3 & \mathbf{A}_4 \end{bmatrix}^{-1} = \left[\begin{array}{c|c} \mathbf{H}_{new}^{old} & -\mathbf{H}_{new}^{old} \mathbf{r}_o \\ \hline (0 & 0 & 0) & 1 \end{array} \right]$$

53



Manipulator Maneuvering Spaces

Joint space: Vector of joint variables, e.g.,

$$\mathbf{r}_J = \begin{bmatrix} \theta_{waist} & \theta_{shoulder} & \theta_{elbow} & \theta_{wrist-bend} & \theta_{flange} & \theta_{wrist-twist} \end{bmatrix}^T$$

End-effector space: Vector of end-effector positions, e.g.,

$$\mathbf{r}_E = \begin{bmatrix} x_{tool} & y_{tool} & z_{tool} & \psi_{tool} & \theta_{tool} & \phi_{tool} \end{bmatrix}^T$$

Task space: Vector of task-dependent positions, e.g., locating a symmetric grinding tool above a horizontal surface:

$$\mathbf{r}_T = \begin{bmatrix} x_{tool} & y_{tool} & z_{tool} & \psi_{tool} & \theta_{tool} \end{bmatrix}^T$$

54

Forward and Inverse Transformations of a Robotic Assembly

Forward Transformation

Transforms homogeneous coordinates from tool frame to reference frame coordinates

$$\begin{aligned} s_{base} &= \mathbf{A}_{tool}^{base} s_{tool} \\ &= \mathbf{A}_{waist} \mathbf{A}_{shoulder} \mathbf{A}_{elbow} \mathbf{A}_{wrist-bend} \mathbf{A}_{flange} \mathbf{A}_{wrist-twist} s_{tool} \end{aligned}$$

Inverse Transformation

Transform homogeneous coordinate from reference frame to tool frame coordinates

$$\begin{aligned} s_{tool} &= \mathbf{A}_{base}^{tool} s_{base} \\ &= \mathbf{A}_{wrist-twist}^{-1} \mathbf{A}_{flange}^{-1} \mathbf{A}_{wrist-bend}^{-1} \mathbf{A}_{elbow}^{-1} \mathbf{A}_{shoulder}^{-1} \mathbf{A}_{waist}^{-1} s_{base} \end{aligned}$$

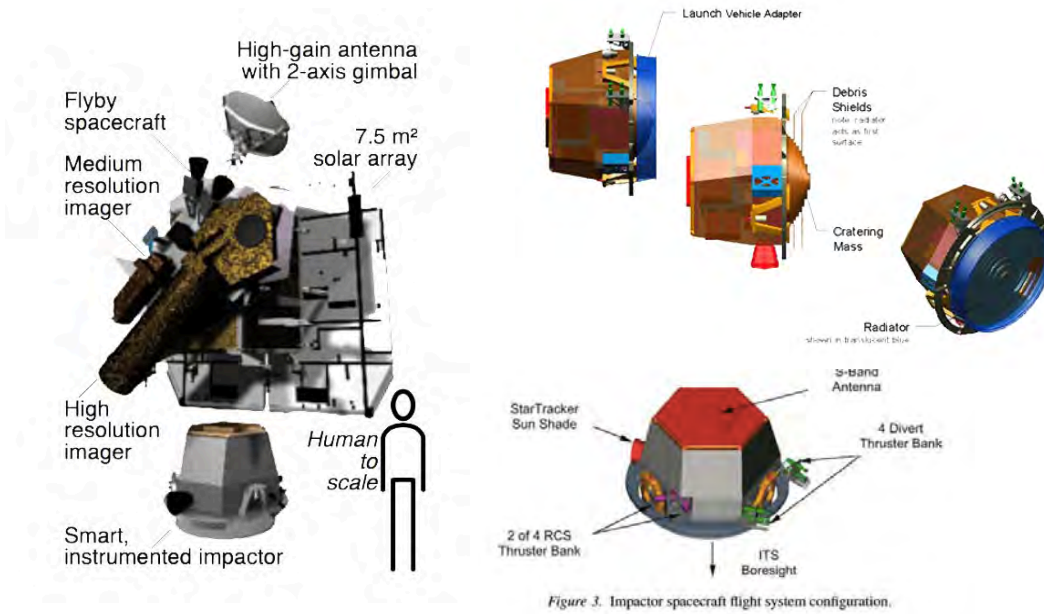
55

Deep Impact 1



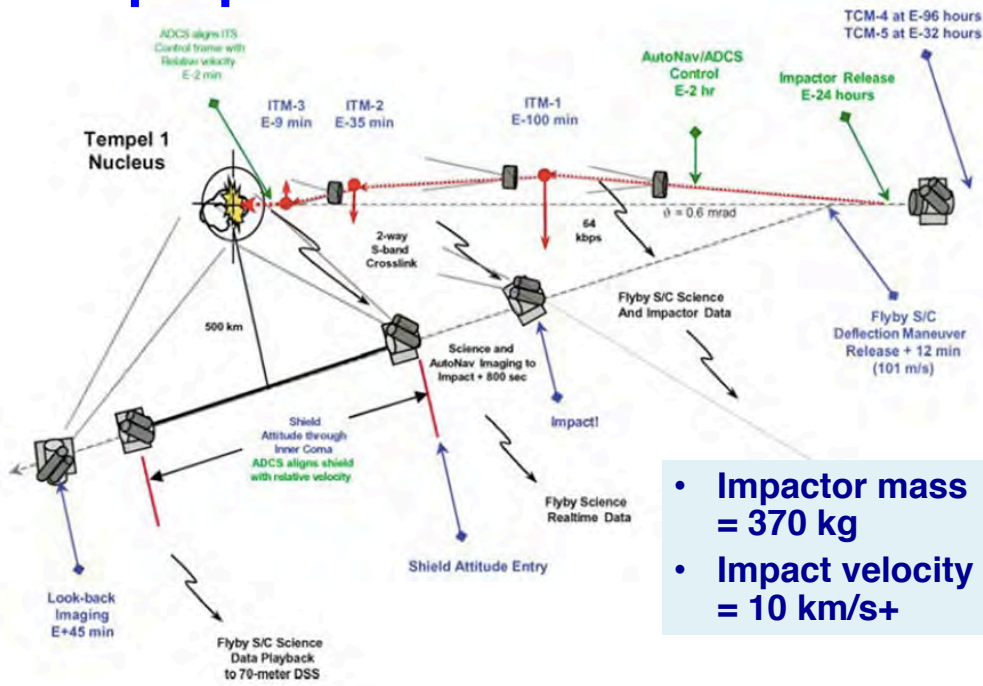
56

Deep Space 1 Flyby and Impactor Spacecraft



57

Deep Space 1 Encounter Scenario



58

Impactor Characteristics

- Image data volume:
 - 17 MB (~35 images)
- Pointing accuracy:
 - $3\sigma = 2$ mrad
- Energy storage for 24-hr mission:
 - 28 KWh
- Propulsion/RCS:
 - 25 m/s divert, 1750 N-s impulse

59

Deep Space 1 Autonomous Navigation and Targeting

- Flyby spacecraft comes within 500 km of Tempel 1 comet, observes impact event for 800 s
- Impactor guided toward comet nucleus by *AutoNav* software (s/w)
- Identical attitude determination and control (*ADCS*) s/w in Flyby and Impactor
- Impactor Targeting Sensor (*ITS*) commands images every 15 sec
- “*Scripted Autonomy*”

Mastrodemos, Kubitschek, Synnott, JPL, 2005

60

Flyby Flight Control System

- Two RAD750 computers
- Medium Resolution Imager (*MRI*) for autonomous navigation during encounter
- High Resolution Imager (*HRI*) for approach phase optical navigation
- Power to both s/c while attached
- High-gain antenna for data return
- S-band antenna for communication with Impactor
- 3-axis momentum wheel attitude control
- 4 RCS thrusters for divert and momentum dumps
- Star Tracker/Inertial Reference Unit (*SSIRU*)

Mastrodemos, Kubitschek, Synnott, JPL, 2005

61

Impactor Flight Control System

- Battery power for 24-hr operation
- One RAD750 computer
- SSIRU
- Simple ITS
- Divert/RCS thrusters
- *AutoNav* components
 - Image processing
 - Orbit determination
 - Maneuver computation

Mastrodemos, Kubitschek, Synnott, JPL, 2005

62

Impactor Targeting Strategy

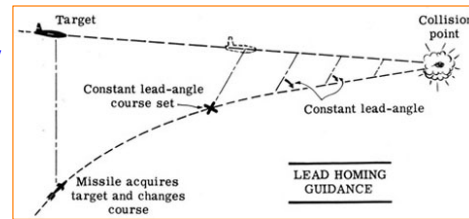
- Options

- **Proportional Navigation**

- Measurement of closing velocity and line-of-sight angular rates
 - “Reduced dynamic approach”

- **Predictive Guidance**

- Equations of motion for target and interceptor
 - State estimation (“filtering”), like **SLAM**



- Selected: Predictive, Pulsed Guidance to desired location on target
- Best quality observations obtained during non-thrusting periods

Mastrodemos, Kubitschek, Synnott, JPL, 2005

63

Impactor Targeting Strategy

- Large uncertainty in knowledge of prior position reduced via optical navigation
- Nucleus rotation rate and solar phase angle induce motion in center of brightness (**CB**)
- Mitigated by batch filtering process and selection of 20-min data arc length

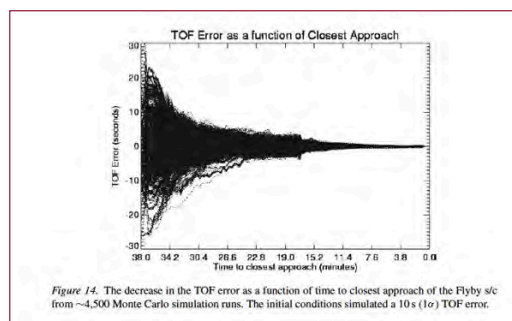


Figure 14. The decrease in the TOF error as a function of time to closest approach of the Flyby s/c from ~4,500 Monte Carlo simulation runs. The initial conditions simulated a 10s (1σ) TOF error.

Mastrodemos, Kubitschek, Synnott, JPL, 2005

64

Autonomous Navigation

- **AutoNav modes**
 - Star-relative mode
 - Star-less mode based on *ADCS* only and camera alignment
- **Autonomous guidance process**
 - 1) $T_{\text{impact}} - 2 \text{ hr}$: Acquire comet nucleus images every 15 sec
 - 2) Compute pixel/line location of *CB*
 - 3) Compute measurement error
 - 4) Perform trajectory observation (*OD*) updates every min
 - 5) Perform 3 Impactor targeting maneuvers (*ITM*), at $T_{\text{impact}} - 100 \text{ min}$, $T_{\text{impact}} - 35 \text{ min}$, $T_{\text{impact}} - 7.5 \text{ min}$
 - 6) Compute scene-analysis-based offset prior to 3rd *ITM*
 - 7) $T_{\text{impact}} - 4 \text{ min}$: Point *ITS* along estimated comet-relative velocity vector
 - 8) Flyby maintains tracking of impact point

Mastrodemos, Kubitschek, Synnott, JPL, 2005

65

Trajectory Determination

- Updated once per minute for last 2 hr
- Sequential batch processing updates position, velocity, navigation line-of-sight attitude bias drift errors
- 80 observations in each 20-min arc
- Time series of Impactor position relative to the nucleus predicted with *Chebyshev polynomial* (i.e., smooth extrapolation of prior position estimates)



Mastrodemos, Kubitschek, Synnott, JPL, 2005

66

Impactor Targeting Maneuvers (ITM)

- Initiated via *AutoNav* sequence command
- Required impulsive maneuver ΔV magnitude and direction calculated
- Finite-burn start time computed, t_{start}
- Integration of accelerometer data indicates when ΔV has been reached, and burn is terminated, t_{finish}
- *ITM-1* removes Flyby pre-release delivery errors (~ 6 km), requiring $\Delta V \sim 1$ m/s
- *ITM-2* improves targeting, requiring $\Delta V \sim 11$ cm/s
- *ITM-3* refines fine targeting of illuminated nucleus based on *CB* observations, requiring $\Delta V \sim 7$ m/s
 - B-plane correction of as much as 4 km
 - Accurate to ~ 54 m

Mastrodemos, Kubitschek, Synnott, JPL, 2005

67

Expected Targeting Error

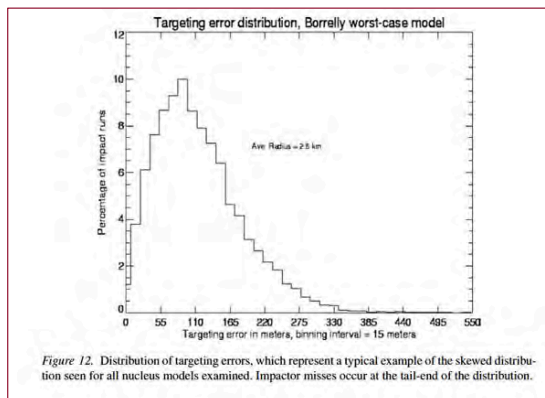
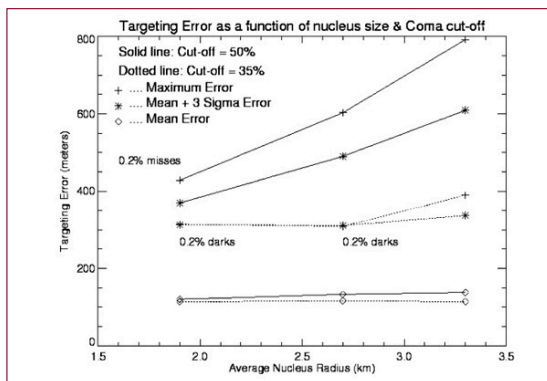
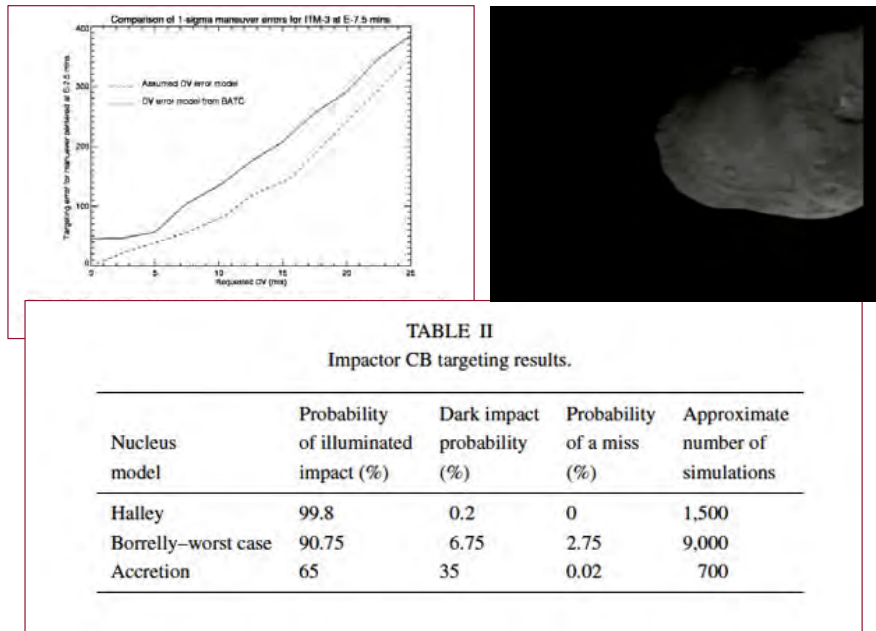


Figure 12. Distribution of targeting errors, which represent a typical example of the skewed distribution seen for all nucleus models examined. Impactor misses occur at the tail-end of the distribution.

Mastrodemos, Kubitschek, Synnott, JPL, 2005

68

Expected Targeting Error



Mastrodemos, Kubitschek, Synnott, JPL, 2005

69

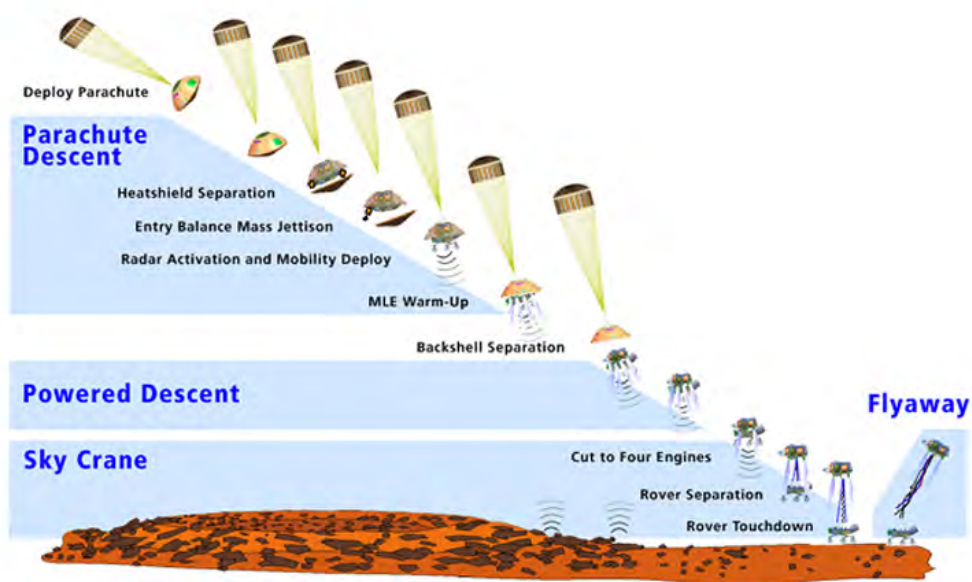
*Next Time:
Human Factors of
Spaceflight*

70

Supplemental Material

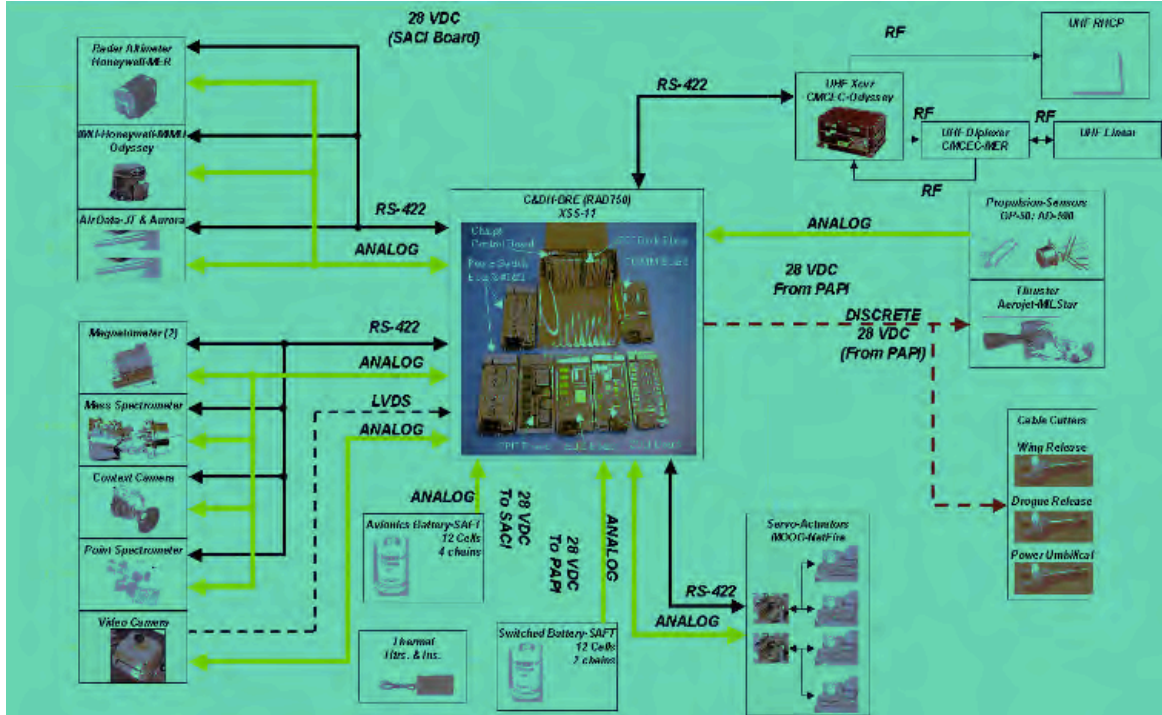
71

MSL Descent



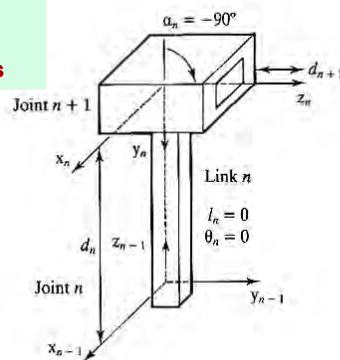
72

ARES Data Handling and Processing System



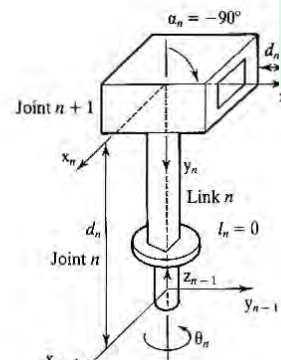
Links Involving Prismatic Joints

Type 5 Link
Intersecting
prismatic joints

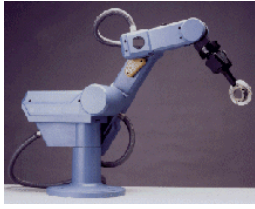


- Link n extends along z_{n-1} axis
 - $l_n = 0$, along x_{n-1}
 - $d_n = \text{length, along } z_{n-1} \text{ (variable)}$
 - $\theta_n = 0$, about z_{n-1}
 - $\alpha_n = \text{fixed orientation of } n+1 \text{ prismatic axis about } x_{n-1}$

Type 6 Link
Intersecting revolute
and prismatic joints

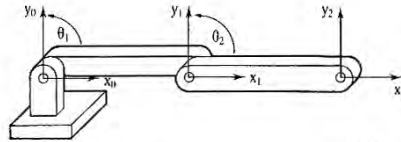


- Link n extends along z_{n-1} axis
 - $l_n = 0$, along x_{n-1}
 - $d_n = \text{length, along } z_{n-1} \text{ (fixed)}$
 - $\theta_n = \text{variable joint angle } n \text{ about } z_{n-1}$
 - $\alpha_n = \text{fixed orientation of } n+1 \text{ prismatic axis about } x_{n-1}$

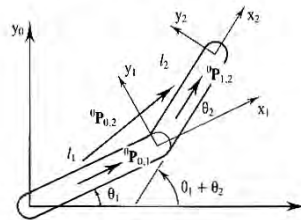


Two-Link/Three-Joint Manipulator

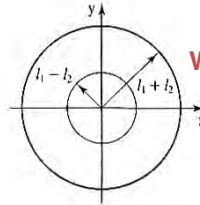
Parallel Rotation
Axes



Manipulator in
zero position



Assignment of
coordinate frames



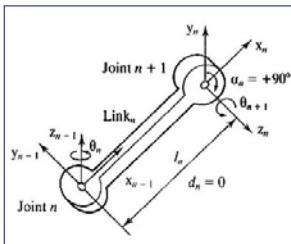
Workspace

Parameters and Variables for
2-link manipulator

- Link lengths (fixed)
- Joint angles (variable)

McKerrow, 1991

75



Denavit-Hartenberg Representation of Joint-Link-Joint Transformation

- Like Euler angle rotation, transformational effects of the 4 link parameters are defined in a **specific application sequence** (right to left): $\{\theta, d, l, \alpha\}$

4 link parameters

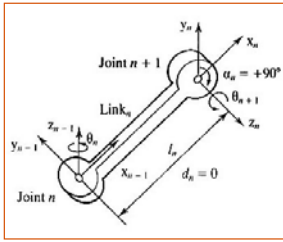
- Angle between 2 links, θ (revolute)
- Distance (offset) between links, d (prismatic)
- Length of the link between rotational axes, l , along the common normal (prismatic)
- Twist angle between axes, α (revolute)

$$\begin{aligned} A_n &= A(z_{n-1}, \theta_n) A(z_{n-1}, d_n) A(x_{n-1}, l_n) A(x_{n-1}, \alpha_n) \\ &= \text{Rot}(z_{n-1}, \theta_n) \text{Trans}(z_{n-1}, d_n) \text{Trans}(x_{n-1}, l_n) \text{Rot}(x_{n-1}, \alpha_n) \\ &\triangleq {}^nT_{n+1} \quad \text{in some references (e.g., McKerrow, 1991)} \end{aligned}$$

Denavit-Hartenberg Demo

<http://www.youtube.com/watch?v=10mUtjfGmzw>

76



Four Transformations from One Joint to the Next (Single Link)

Rotation of θ_n about the z_{n-1} axis

$$\text{Rot}(z_{n-1}, \theta_n) = \begin{bmatrix} \cos \theta_n & -\sin \theta_n & 0 & 0 \\ \sin \theta_n & \cos \theta_n & 0 & 0 \\ 0 & 0 & 1 & 0 \\ 0 & 0 & 0 & 1 \end{bmatrix}$$

Translation of d_n along the z_{n-1} axis

$$\text{Trans}(z_{n-1}, d_n) = \begin{bmatrix} 1 & 0 & 0 & 0 \\ 0 & 1 & 0 & 0 \\ 0 & 0 & 1 & d_n \\ 0 & 0 & 0 & 1 \end{bmatrix}$$

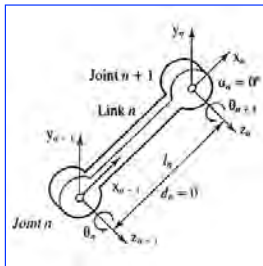
Translation of l_n along the x_{n-1} axis

$$\text{Trans}(x_{n-1}, l_n) = \begin{bmatrix} 1 & 0 & 0 & l_n \\ 0 & 1 & 0 & 0 \\ 0 & 0 & 1 & 0 \\ 0 & 0 & 0 & 1 \end{bmatrix}$$

Rotation of α_n about the x_{n-1} axis

$$\text{Rot}(x_{n-1}, \alpha_n) = \begin{bmatrix} 1 & 0 & 0 & 0 \\ 0 & \cos \alpha_n & -\sin \alpha_n & 0 \\ 0 & \sin \alpha_n & \cos \alpha_n & 0 \\ 0 & 0 & 0 & 1 \end{bmatrix}$$

77



Joint Variable = θ_n

θ = variable
 $d = 0$ m
 $l = 0.25$ m
 $\alpha = 90$ deg

$\theta \triangleq 30$ deg
 $d = 0$ m
 $l = 0.25$ m
 $\alpha = 90$ deg

Example: Denavit-Hartenberg Representation of Joint-Link-Joint Transformation for Type 1 Link

$$\mathbf{A}_n = \begin{bmatrix} \cos \theta_n & -\sin \theta_n \cos \alpha_n & \sin \theta_n \sin \alpha_n & l_n \cos \theta_n \\ \sin \theta_n & \cos \theta_n \cos \alpha_n & -\cos \theta_n \sin \alpha_n & l_n \sin \theta_n \\ 0 & \sin \alpha_n & \cos \alpha_n & d_n \\ 0 & 0 & 0 & 1 \end{bmatrix}$$

$$\mathbf{A}_n = \begin{bmatrix} \cos \theta_n & 0 & \sin \theta_n & 0.25 \cos \theta_n \\ \sin \theta_n & 0 & -\cos \theta_n & 0.25 \sin \theta_n \\ 0 & 1 & 0 & 0 \\ 0 & 0 & 0 & 1 \end{bmatrix}$$

$$\mathbf{A}_n = \begin{bmatrix} 0.866 & 0 & 0.5 & 0.217 \\ 0.5 & 0 & -0.866 & 0.125 \\ 0 & 1 & 0 & 0 \\ 0 & 0 & 0 & 1 \end{bmatrix}$$

78

Matrix Inverse Identity

Given: a square matrix, **A**, and its inverse, **B**

$$\mathbf{A} = \left[\begin{array}{c|c} \mathbf{A}_1 & \mathbf{A}_2 \\ \hline \mathbf{A}_3 & \mathbf{A}_4 \end{array} \right] \begin{matrix} m \times m & m \times n \\ n \times m & n \times n \end{matrix} ; \quad \mathbf{B} \triangleq \mathbf{A}^{-1} = \left[\begin{array}{c|c} \mathbf{B}_1 & \mathbf{B}_2 \\ \hline \mathbf{B}_3 & \mathbf{B}_4 \end{array} \right]$$

Then

$$\mathbf{AB} = \mathbf{AA}^{-1} = \mathbf{I}_{m+n}$$

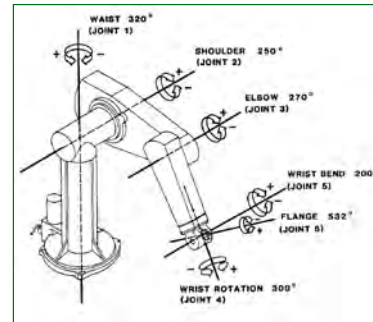
$$= \left[\begin{array}{c|c} \mathbf{I}_m & \mathbf{0} \\ \hline \mathbf{0} & \mathbf{I}_n \end{array} \right] = \left[\begin{array}{c|c} (\mathbf{A}_1\mathbf{B}_1 + \mathbf{A}_2\mathbf{B}_3) & (\mathbf{A}_1\mathbf{B}_2 + \mathbf{A}_2\mathbf{B}_4) \\ \hline (\mathbf{A}_3\mathbf{B}_1 + \mathbf{A}_4\mathbf{B}_3) & (\mathbf{A}_3\mathbf{B}_2 + \mathbf{A}_4\mathbf{B}_4) \end{array} \right]$$

Equating like parts, and solving for \mathbf{B}_i

$$\left[\begin{array}{c|c} \mathbf{B}_1 & \mathbf{B}_2 \\ \hline \mathbf{B}_3 & \mathbf{B}_4 \end{array} \right] = \left[\begin{array}{c|c} (\mathbf{A}_1 - \mathbf{A}_2\mathbf{A}_4^{-1}\mathbf{A}_3)^{-1} & -\mathbf{A}_1^{-1}\mathbf{A}_2(\mathbf{A}_4 - \mathbf{A}_3\mathbf{A}_1^{-1}\mathbf{A}_2)^{-1} \\ \hline -\mathbf{A}_4^{-1}\mathbf{A}_3(\mathbf{A}_1 - \mathbf{A}_2\mathbf{A}_4^{-1}\mathbf{A}_3)^{-1} & (\mathbf{A}_4 - \mathbf{A}_3\mathbf{A}_1^{-1}\mathbf{A}_2)^{-1} \end{array} \right]$$

79

Forward and Inverse Kinematics Between Joints, Tool Position, and Tool Orientation



Forward Kinematic Problem: Compute the **position of the tool** in the reference frame that corresponds to a given joint vector (i.e., vector of link variables)

$$\mathbf{s}_{base} = \mathbf{A}_{waist} \mathbf{A}_{shoulder} \mathbf{A}_{elbow} \mathbf{A}_{wrist-bend} \mathbf{A}_{flange} \mathbf{A}_{wrist-twist} \mathbf{s}_{tool} = \mathbf{A}_{tool}^{base} \mathbf{s}_{tool}$$

To Be Determined \Leftarrow Given

Inverse Kinematic Problem: Find the **vector of link variables** that corresponds to a desired task-dependent position

$$\mathbf{A}_{waist} \mathbf{A}_{shoulder} \mathbf{A}_{elbow} \mathbf{A}_{wrist-bend} \mathbf{A}_{flange} \mathbf{A}_{wrist-twist} \mathbf{s}_{tool} = \mathbf{A}_{tool}^{base} \mathbf{s}_0 = \mathbf{s}_{base}$$

To Be Determined \Leftarrow Given

80